Modelling of Dislocation Mobility Controlled Brittle-to-Ductile Transition

Valerie R. Nitzsche and K. Jimmy Hsia

Department of Theoretical and Applied Mechanics
University of Illinois at Urbana-Champaign, Urbana, IL 61801, USA

Abstract

The phenomenon of brittle-to-ductile transition (BDT) is known to be controlled by the competition between cleavage fracture and dislocation activity at crack tips. But the transition could be determined by one of the two successive processes, dislocation nucleation, or dislocation motion. In this paper a model is developed to study the BDT controlled by dislocation mobility. The model material is assumed to undergo elastic-rate dependent plastic deformation with the plastic strain rate scaled with dislocation velocity. An isotropic plasticity theory is used. The BDT is assumed to occur when the crack tip is shielded by the surrounding plastic zone such that it never reaches the critical stress intensity for cleavage fracture. The crack tip shielding due to plastic deformation is evaluated using the finite element method. The dimensionless groups which affect the BDT are identified, and a parametric study is performed to reveal the effects of various dimensionless parameters. Numerical results using the specific material properties of Si single crystals are compared with experimental data. Good agreements are obtained. Some interesting features of the BDT behavior are predicted by our computer simulations which require further confirmation by experimental studies.

I. Introduction

The transition of fracture behavior in many crystalline solids from a high energy absorbing ductile mode to a very low energy absorbing cleavage mode is an important constraint in their use as structural materials. Of particular importance are those application in which the structures are subjected to relatively low temperatures and high strain rates. Although it is generally agreed that brittle-to-ductile transition (BDT) is the result of the competition between dislocation activity and cleavage fracture at crack tips, this phenomenon is still not well understood mechanistically. Since the pioneering model of Rice and Thomson [1], in which an activation analysis of dislocation nucleation from a sharp crack tip was performed, much experimental and theoretical effort has been made. However, controversy still exists as to whether the BDT is dislocation emission controlled or dislocation motion controlled [2,3,4]. Furthermore, it is not yet clear what the relationships are between: 1) the transition temperature and strain rate (loading rate), 2) the transition temperature and crack tip configuration (crack orientation with respect to crystallographic orientation), and 3) the transition temperature and loading conditions (Mode I or mixed mode, tensile or bending loading).

The answers to these questions obviously depend on the material system being considered. Even for simple material systems, such as single crystalline b.c.c. metals or ceramic and semiconductor materials such as *MgO* and *Si* crystals, many other factors could still affect the controlling mechanisms of BDT. Such factors could range from whether there are pre-existing dislocations in the crystal to whether there exist dislocation nucleation sites other than the crack tip to whether impurity in the material affects dislocation mobility. To avoid ambiguity, a clean material, *Si* single crystal, has widely been selected for experimental study of the fundamental mechanisms of BDT.

The first mechanistic experimental study of *Si* was conducted by St. John [5] in which fracture stress was measured in a tapered cantilever beam specimen at various loading rates and temperatures. Brede and Haasen [6], and Michot [7] used similar techniques and studied the effects of doping on the BDT temperature. Samuels and Roberts [8] used a four point bending specimen with an indentation surface crack in which the available slip planes and dislocation configurations around the crack front were significantly different from those of the other studies. Most recently, Brede et al [3] and Hsia and Argon [9] studied the BDT of a propagating crack in a temperature gradient field. The following interesting observations, though not always consistent, were obtained by these experimental studies of *Si* single crystals. The BDT was found to be very sharp and usually occurred within a few degrees Celsius in all experiments. The transition temperature increases with increasing loading rate for tests on stationary cracks [5,6,7,8]. For very similar materials (similar doping concentration and crystal growth technique) under comparable loading rate even though the slope of $\log(\dot{K})$ versus $1/T_c$ curve

remains nearly constant, the BDT temperature can be drastically different for different loading types (e.g., four point bending tests [8] versus double cantilever beam tests, see Figure 3 in [4]). Therefore, the BDT behavior is structure sensitive. In these experiments the crack propagation often exhibited an unsteady, jittery manner (alternating jumps and stops) at both room temperatures and elevated temperature [3,6,9].

A particularly interesting observation is that the applied stress intensity at fracture increases slightly at high temperatures, especially at temperatures within about 100°C of the BDT temperature, as shown schematically in Fig. 1. The increasing rate levels off as the temperature approaches the transition temperature and shoots up suddenly at the BDT temperature. This abrupt increase characterizes the change of fracture behavior from brittle to ductile mode. The level of increase in fracture stress below the BDT ranges from about 15% [8] to sometimes more than 100% [6], and is dependent on the loading rate. This observation can be explained if one argues that dislocation nucleation is substantially easier than dislocation motion near the transition temperature. Thus, dislocations would be nucleated at a temperature lower than the BDT temperature. However, their mobility may not be high enough to result in enough crack tip shielding to bring about the transition. Nevertheless, the emission of these dislocations and their travelling away from crack tips for a few Burgers vectors could be enough to increase the applied stress intensity at fracture by more than 15%. Some experimental evidence exists for *Si* [3,9] and other materials [10] which shows that the crack continues to grow in a cleavage fashion despite the nucleation of dislocations from the crack tip.

Many models have been developed to describe the BDT behavior of single crystals. These models can be broadly categorized into two groups: those which consider dislocation nucleation as the controlling mechanism for the BDT [1,11-13], and those which consider dislocation motion as the controlling mechanism for the BDT [2,4,14-16]. The models with dislocation nucleation as the controlling mechanism characterize materials as either brittle or ductile with a very clear cut criterion, but they suffer from their inability to predict the right BDT temperature and the loading rate dependence of the BDT temperature. On the other hand, those models with dislocation motion as the controlling mechanism can usually predict a loading rate dependency of the BDT temperature. However, except for a recent model by Hirsch and Roberts [4], a sharp transition could not be predicted by these models. Furthermore, most of these models consider the detailed configurations of dislocations near the crack tip and their shielding effects on the crack tip stress intensity at an atomistic level, but they are unable to evaluate the potential effects of dislocation motion on the surrounding stress fields. It is expected that the rate dependent plastic deformation due to dislocation motion would not only shield

the crack tip from reaching the critical stress intensity, but also alter the stress distribution around the crack tip region.

In the present communication, we develop a model for BDT controlled by dislocation mobility. The material is assumed to undergo elastic deformation and a rate-dependent plastic deformation induced by dislocation motion. The crack tip shielding due to the plastic deformation is evaluated numerically using the finite element method so that the evolution of the crack tip fields can be accurately modelled. The dimensionless groups controlling the BDT behavior are identified by dimensional considerations, and parametric studies are performed to reveal the effects of different parameters. In particular, the effects of temperature, loading rate, and power law stress exponent are investigated. The numerical results show good agreement with the experimental data of Brede and Haasen [6] for *Si* single crystals. Some interesting features of the BDT are predicted by this numerical study which require further experimental confirmation.

II. Dislocation Mobility Controlled Model

The basic premise of this model is that the BDT is controlled by dislocation mobility. This implies that dislocation nucleation is substantially easier than dislocation motion around the BDT temperature, and that nucleation could occur at a temperature lower than the transition temperature and at a stress intensity lower than the critical stress intensity. The rate-dependent plastic deformation is then solely due to the motion of these dislocations.

For simplicity, we assume that the material behavior is isotropic. Real single crystalline materials are generally anisotropic. Since dislocation motion only occurs on a limited number of slip planes, plastic deformation in single crystals is always anisotropic. However, the effects of crack tip shielding due to dislocation motion in single crystals could be similar to that of plastic deformation in isotropic materials. Furthermore, in the present model, a stationary crack under different loading rates is considered, therefore no elastic unloading due to crack propagation occurs.

2.1 Material Constitutive Behavior

For plastic deformation due to dislocation motion, the inelastic shear strain rate, $\dot{\gamma}^p$, can be given by,

$$\dot{\gamma}^p = \beta \rho b v, \tag{1}$$

where β is a proportionality constant, ρ is the dislocation density, b is the magnitude of the Burgers vector of a dislocation, and v is the dislocation velocity. The dislocation velocity in single crystals is usually found to be related to the resolved shear stress, τ, and obey an Arrhenius type law, as

$$v = v_0 exp\left(-\frac{Q}{kT}\right)\left(\frac{\tau}{\tau_0}\right)^n, \tag{2}$$

where v_0 and τ_0 are material specific reference dislocation velocity and reference shear stress, Q is the activation energy for dislocation motion, k is the Boltzmann's constant, T is the absolute temperature in degrees Kelvin, and n is the power law exponent which is a material constant for a wide range of stress levels. Substituting equation (2) for v in equation (1) gives

$$\dot{\gamma}^p = \dot{\gamma}_0 exp\left(-\frac{Q}{kT}\right)\left(\frac{\tau}{\tau_0}\right)^n, \tag{3}$$

where $\dot{\gamma}_0$ is a reference shear strain rate and is a function of the dislocation density ρ and the Burgers vector b. For an isotropic material there is no preferred slip plane. Therefore, the resolved shear stress τ and plastic shear strain rate $\dot{\gamma}^p$ in equation (3) can be replaced by the von Mises equivalent stress σ and the equivalent strain rate $\dot{\varepsilon}^p$. The viscoplastic response of the material can then be modelled as,

$$\dot{\varepsilon}^p = \dot{\varepsilon}_0 exp\left(-\frac{Q}{kT}\right)\left(\frac{\sigma}{\sigma_0}\right)^n, \tag{4}$$

where $\dot{\varepsilon}_0$ is a reference strain rate, and σ_0 is a reference stress.

For a given material, the value of n can be determined from a plot of dislocation velocity versus applied stress at a specific temperature (e.g., from Fig. 3.11 in Ref [17]). The activation energy, Q, for dislocation motion can be obtained from $log(v)$ versus T plots (e.g., Fig.3.10b in Ref. [17]).

The total strain in the material consists of an elastic strain and a plastic strain. It is assumed, as in all other theories, that the elastic and plastic strains are additive. Thus the total strain rate, $\dot{\varepsilon}$, is given by,

$$\dot{\varepsilon} = \dot{\varepsilon}^e + \dot{\varepsilon}^p, \tag{5}$$

where $\dot{\varepsilon}^e$ is the elastic strain rate, and is given in terms of the changing rate of the stresses and the Young's modulus E and Poisson's ratio ν by the generalized Hooke's law for an isotropic material.

2.2 Some Dimensional Considerations

For an atomically sharp crack under a far field applied stress intensity K^{app}, the rate-dependent plastic deformation due to dislocation motion provides crack tip shielding. Therefore, unless the applied loading rate is extremely high or the temperature is very low, the crack tip stress intensity K^{tip} could be substantially lower than the applied stress intensity K^{app}.

Generally, the crack tip stress intensity is a function of the material parameters, temperature, loading rate, and time, t, as,

$$K_I^{tip} = f(\dot{K}_I^{app}, K_I^{app}, T, E, \upsilon, Q, \sigma_0, \dot{\varepsilon}_0, n, D, t), \quad (6)$$

where D is a characteristic dimension of the model which will be discussed in the next section. It is noted that σ_0 and $\dot{\varepsilon}_0$ are not independent material constants and can only be determined from experimental data as the combination, $\dot{\varepsilon}_0\sigma_0^{-n}$.

We define two reference quantities for dimensional considerations. One is a reference length which roughly represents the plastic zone size at fracture,

$$R_0 \equiv \frac{1}{2\pi}\left(\frac{K_{Ic}}{\sigma_0}\right)^2, \quad (7)$$

where K_{Ic} is the material's critical stress intensity. The other is a characteristic time defined as,

$$t_c \equiv \alpha\frac{\sigma_0/E}{\dot{\varepsilon}_0}, \quad (8)$$

where α is a dimensionless coefficient which can be used to fit the experimental data.

From dimensional considerations, for a constant rate of applied mode I stress intensity, $\dot{K}_I^{app}$=constant, the crack tip stress intensity can then be given by,

$$\frac{K_I^{tip}(t)}{K_{Ic}} = \frac{K_I^{app}(t)}{K_{Ic}} \times g\left(\frac{\dot{K}_I^{app}}{K_{Ic}/t_c}, \frac{Q}{kT}, \frac{\sigma_0}{E}, \nu, n, \frac{D}{R_0}\right). \quad (9)$$

The dimensionless quantities in equation (9) will collectively determine the ratio of the crack tip stress intensity to the applied stress intensity, thus determining the brittle to ductile transition temperature.

2.3 Fracture Criterion and Brittle-to-Ductile Transition

Cleavage fracture is assumed to occur when the crack tip stress intensity reaches the intrinsic fracture toughness of the material, i.e.,

$$K_I^{tip} = K_{Ic}. \quad (10)$$

In reality, this fracture criterion is not exactly true when there are many dislocations emitted from the crack tip. Dislocation emission from the crack tip will bring about a tortuous crack front and

possibly crack tip blunting [9], which would result in a critical stress intensity slightly higher than the intrinsic fracture toughness. However, the relationship between dislocation generation and the increase in the critical stress intensity is not known. Thus, it can not be modelled accurately.

Generally, at high loading rates and low temperatures, fracture occurs when $K_I^{app} \approx K_{Ic}$. For a given loading rate, as the temperature increases, due to the increasing shielding effect, the crack tip stress intensity will reach K_{Ic} at a higher applied stress intensity. Beyond a critical temperature, regardless of the level of K_I^{app}, the K_I^{tip} never reaches the critical stress intensity. In our model, this critical temperature is defined as the BDT temperature T_c for the given loading rate.A similar definition was used by Hirsch et al [15] and Brede [16].

III. Model for Numerical Analysis

To study the effect of shielding by rate-dependent plasticity, the finite element method is used. The problem we would encounter with this method is that, for an elastic/rate-dependent plastic material, the transient crack tip field under far field constant loading rate may not be characterized by the stress intensity factor. Riedel and Rice [18] showed that, for elastic-power law creeping materials under a step-function loading at t=0, the crack tip stress distribution rapidly changes from $1/\sqrt{r}$ singularity to an HRR type singularity [19,20] during the transient stage. Moreover, the transient response at a stationary crack tip is such that neither the J-integral [21] nor the C-integral [22,23] is path-independent. Because of this, the crack tip stress intensity is ill-defined during the transient loading stage and can not be calculated properly by the finite element method.

To overcome this difficulty, the elastic zone concept, developed by Suo et al [24] to deal with cleavage fracture in the presence of background plasticity, was adopted. A circular elastic region (elastic zone) of radius D, shown in Fig. 2a, was introduced at the crack tip. This zone allowed crack tip stress intensity at any instant during loading to be evaluated without ambiguity. The physical interpretation of the elastic zone is that, within a small distance from the crack tip, the dislocation activity there can not be treated by a continuum theory. The plastic deformation process at this length scale is in fact discrete. Furthermore, the effect of the dislocations infinitely close to a crack tip on the shielding of the crack tip is not well understood. Most atomistic models which consider the contributions of individual dislocations have defined a critical distance away from the crack tip for dislocation nucleation. Hirsch et al [15] and Hirsch and Roberts [4] assumed that the condition for nucleation of a new dislocation loop is that the stress at a critical distance x_c from the crack tip must be sufficient to expand the loop against the line tension/image stress resistance. Brede [16], on the other hand, plainly

assumed that dislocations would be emitted at a distance r_0 from the crack tip when the resolved stress on the dislocation exceeded a critical level. In these models, a critical (or characteristic) length could not be avoided. In the present model, the characteristic length is the elastic zone size D, which is usually chosen to be a small fraction of the characteristic plastic zone size R_0 defined in equation (7). The implication of the elastic zone is that, whatever dislocation activities there are within the elastic zone, the effects of them on the crack tip shielding are negligible.

A circular region centered at the crack tip with radius much larger than R_0 was considered in the current study (See Fig. 2). Plane strain, 8-node reduced integration elements were used. A typical finite element mesh is shown in Figure 2b. At the crack tip, a ring of singular elements with a strain singularity of $1/\sqrt{r}$ were used to capture the elastic stress and strain singularities. A circular elastic zone of radius D was introduced by assigning an elastic property to the first few rings of elements around the crack tip. The remainder of the model behaves as an elastic/rate-dependent plastic material obeying the constitutive law of equations (4) and (5). A mode I K-field was applied at the nodes along the outer boundary by imposing displacement boundary conditions. Different constant rates of applied stress intensity were obtained by having different displacement rates along the boundary.

The finite element software, ABAQUS [25], was employed to calculate the response of the cracked body under various loading conditions and temperatures. The J-integral was calculated along several contours within the elastic zone. The crack tip stress intensity was calculated from the J-integral values at any given instant utilizing

$$K_I^{tip} = \left(\frac{JE}{1-\nu^2}\right)^{1/2}. \qquad (11)$$

IV. Results

Computer simulations have been performed to investigate the crack tip shielding due to plastic deformation and the behavior of BDT based on the current model. In this section, the general behaviors of the model for different dimensionless parameters will be studied. Then a specific material, single crystalline silicon, will be studied. The results will be compared with experimental measurements.

4.1 General Behavior for Different Parameters

The typical crack tip shielding effects due to rate-dependent plastic deformation are shown in Fig. 3, where the normalized crack tip stress intensities, K_I^{tip}/K_{Ic}, for a number of different temperatures at a constant loading rate, $\dot{K}_I^{app}/(K_{Ic}/t_c) = 1.0$ are plotted as a function of applied stress inten-

sity, K_I^{app}/K_{Ic}. The material parameters used in this calculation are shown in the figure caption. The plot clearly indicates that because of rate-dependent plastic deformation, the crack tip stress intensity is no longer proportional to the applied stress intensity.

At relatively low temperatures, the relationship between the crack tip stress intensity and the applied stress intensity is nearly linear. As the temperature increases, the dislocation mobility increases according to an Arrhenius law, thus the shielding effects become more substantial. As a result, the crack tip stress intensity would reach K_{Ic} (if it ever reaches K_{Ic}) at a larger K_I^{app} for higher temperatures. Beyond the critical temperature (T_c=1004K in this case), no matter how large the applied stress intensity is, the crack tip stress intensity will not go beyond K_{Ic}. Thus the BDT occurs.

As expected, a very similar behavior is predicted by the current model for different loading rates at a given temperature (The normalized loading rate will be denoted by $\dot{\bar{K}} \equiv \dot{K}_I^{app}/(K_{Ic}/t_c)$ hereafter). Fig. 4 shows the results of the K_I^{tip}/K_{Ic} versus K_I^{app}/K_{Ic} curves for different loading rates at T=1000K. Although the material could be brittle under a high loading rate at this temperature, it could become ductile under a lower loading rate.

The BDT temperature as a function of loading rate is illustrated in Fig. 5, in which the applied stress intensity required for cleavage fracture, K_{Ic}^{app}, is plotted as a function of temperature for several different loading rates. It is seen that for all the loading rates considered, the BDT is rather sharp. The required far field stress intensity for fracture increases dramatically within a few degrees of the transition temperature. However, our computer simulation results also show that within a wide temperature range below the transition temperature (often more than 100 to 150K), there is a steady increase in the apparent fracture toughness of about 50-200% due to dislocation activities at the crack tip. Nevertheless, the crack tip shielding due to the motion of these dislocations is just not enough to prevent the crack from fracturing in a brittle, cleavage fashion. Fig. 5 also shows that the increase in the apparent fracture toughness depends upon the loading rate. This will be discussed further later.

The effect of the stress exponent n was also investigated. As n becomes larger, the plastic strain rate becomes increasingly sensitive to the stress level. For very large n, a stress $\sigma>\sigma_0$ will produce a very high plastic strain rate, whereas $\sigma<\sigma_0$ will result in a negligible plastic strain rate. This effect is shown in Fig. 6 where the apparent fracture toughness is plotted as a function of temperature for three different n values. In calculating these curves, the coefficient α in equation (8) for different n was adjusted such that different n values would give the same transition temperature at a specific loading rate ($\dot{\bar{K}}$=1). The determined α value was then used for the other loading rates for a given exponent n. Fig. 6 shows that the relation between the BDT temperature and the loading rate does not

depend on the n value. But as n increases, because of the higher sensitivity of the plastic strain rate on the stress, the transition becomes sharper. For n=1.4, a toughening (increase in apparent fracture toughness) of 100-200% was obtained before the BDT occurred. But for n=10, only a 20-40% increase in the apparent fracture toughness was achieved. This effect is also shown in Fig.7 where the K_I^{tip}/K_{Ic} versus K_I^{app}/K_{Ic} curves for a few n values are plotted around the BDT temperature. While the crack tip stress intensity for n=1.4 approaches the critical stress intensity in a very gradual manner, the crack tip stress intensity for n=10 increases nearly linearly until just below the critical stress intensity and then turns abruptly. We will discuss the implications of this behavior further later.

4.2 Comparison with Experimental Results in *Si* Single Crystals

The predictions of the model have been compared with experimental results. Single crystal *Si* was chosen for comparison because of the vast amount of experimental information available for this material. Most material constants used in the calculations were obtained from Brede and Haasen [6]. The stress exponent n was estimated from Fig. 3.11 in Hull [17]. The only model parameter used to fit the experimental data was the coefficient α in equation (8). In our calculation, α was determined by matching the BDT temperature with the experimental value at a specific loading rate. Once it was determined, the same α was used for the other temperatures and loading rates. The material constants used in the calculation for single crystal *Si* are given in Table 1.

The experimental results of Brede and Haasen [6] were used for the comparison. A number of the loading rates applied in their experiments were considered. The lowest loading rate $\dot{K}$=0.885 was used to determine the α value. The computational results are plotted in an Arrhenius-type graph, Fig. 8, together with the experimental data of Brede and Haasen [6]. The circles are our computational results for the loading rates corresponding to the experimental loading rates. The squares are the experimentally measured BDT temperature at those loading rates. The solid line is the best fit Arrhenius curve to the experimental data. It is clear that our computational results agree with the experimentally measured BDT temperatures very well. This is not surprising because if the BDT is controlled by dislocation mobility, it is expected to scale with the Arrhenius curve characterized by the activation energy Q. This behavior has been observed by many researchers.

We also tried to explore whether the crack tip shielding behavior was captured by our model. Fig. 9 shows the comparison between the model predictions and the experimental data of the apparent fracture toughness, K_{Ic}^{app}, as a function of temperature. Although the exact features of the experimental data are not completely captured, the general trend of crack tip shielding seems to be well modelled. On the other hand, it is noted that for these brittle fracture tests, it is very difficult to get highly consis-

tent experimental results. Fig. 9 shows that in some cases ($\dot{\bar{K}} = 4.14, 8.64$) very little crack tip shielding is observed in the experimentally measured critical stress intensity below the BDT temperature. Whereas in some other cases ($\dot{\bar{K}} = 18.50$), substantial shielding is observed experimentally. Consequently, the model predictions are sometimes higher, and sometimes lower than the experimental data.

V. Concluding Remarks

In the current study, we modelled the BDT behaviors based on the single assumption that the transition is controlled by dislocation mobility. The effects of dislocation motion are accounted for using a simple isotropic rate-dependent plasticity theory. The plastic strain rate is assumed to obey an Arrhenius law with a power law dependence on stresses. Except for a coefficient, the dependence of strain rate on temperature and stress can be uniquely determined from the experimental information of dislocation velocity in particular crystals.

The finite element method was used in this study. Since plastic deformation occurs continuously as the load (or stress intensity) is applied gradually, the nature of the current problem is essentially the transient response of the crack tip fields. Most atomistic models using dislocation theories [2,15,16] consider the interactions between dislocations and the crack tip, but are unable to account for the constantly changing stress field around the crack tip during the transient stage. Our study, however, takes full account of the constantly evolving stress distribution and re-distribution during loading. In fact, our computational results show that at the BDT temperature, the stress distributions for different applied loading rates in the plastic zone are almost identical at a crack tip intensity level near K_{Ic}, as shown in Figure 10. Figure 10 also shows that the high stress singularity is substantially reduced due to the plastic deformation. These results are consistent with atomistic simulations of Brede [16] and Hirsch and Roberts [4], and with experimental observations of Michot and George [26].

The elastic zone concept [24] was adopted in the current model. In addition to the operational purpose of obtaining a consistent evaluation of the crack tip stress intensity, this adoption also has some physical implications. Since no plastic deformation occurs within the elastic zone very near the crack tip, it is implied that dislocation activities very near the crack tip do not have a substantial effect on the crack tip field. Furthermore, the existence of an elastic zone effectively creates a barrier to the onset of plastic deformation. This is equivalent to a barrier to dislocation nucleation. The larger the relative elastic zone size, D/R_0, the more difficult it is to initiate plastic deformation, corresponding to a higher barrier to dislocation nucleation. Considering the fact that the instantaneous nucleation of

dislocations is rarely achievable in BCC transition metals such as α-*Fe* and semiconductors such as *Si*, the introduction of an elastic zone to capture the feature of a nucleation barrier seems to be a logical choice. The effects of different elastic zone sizes are currently under investigation.

A number of interesting features of the BDT behavior have been predicted by the current model. Our computer simulation results show that as the stress exponent n increases, the BDT becomes sharper. Generally speaking, a dislocation nucleation controlled BDT would be much sharper than a dislocation mobility controlled BDT, because the nucleation barrier essentially serves as an on/off valve. For nucleation controlled BDT, before the barrier is overcome, the fracture toughness should be the intrinsic cleavage toughness with no crack tip shielding. Once the nucleation barrier is overcome, since dislocation motion is so much easier, the behavior should be purely ductile. Following this argument, our simulation results indicate that materials with a larger stress exponent n are more likely to obey dislocation nucleation controlled BDT, whereas those with a lower n tend to have a dislocation mobility controlled BDT. It is well known that materials such as *Si*, *Ge*, and *GaAs* have relatively low stress exponents (between 1.4 to 3.0), whereas materials like *Fe-3%Si*, *LiF* and *W* have high stress exponents (between 20 to 40) for dislocation velocity. There is indeed experimental evidence that in *Si*, *GaAs*, and *MgO*, dislocation nucleation is easier than dislocation motion [9,10]. On the other hand, it has been observed that in some materials with high value of n such as *W* single crystals, the BDT is rather gradual [27]. It should be noted that the above model prediction is for materials which are initially dislocation-free, and dislocations can only be nucleated from crack tips. Except for *Si* single crystals, almost all other crystals (unless they have been grown in ideal environment such as in space) have pre-existing dislocations in them. The motion and multiplication of pre-existing dislocations will make the BDT more gradual, as has been shown by Warren [28].

Our computational results also show that the sharpness of the BDT depends on the loading rate. At low loading rates, the transition seems to be very sudden. But at high loading rates, the transition tends to be more gradual (see Fig. 5). Based on the same argument, this prediction seems to indicate that the BDT tends to be dislocation nucleation controlled at low loading rate, and dislocation mobility controlled at high loading rate. This is certainly true for the two limiting cases: quasi-static loading and extremely high loading rate. Under quasi-static loading, as long as dislocations can nucleate, they would always have enough time to move away from the crack tip, thus to result in dislocation nucleation controlled BDT; whereas under extremely high loading rate, dislocation mobility is always the rate limiting process. There is no conclusive experimental evidence to support this prediction of the current model. But a close examination of the results by Michot (see, e.g., Fig. 23 in

Ref. [7]) does reveal that when the loading rate increases, the applied critical stress intensity right before the BDT increases steadily.

Because of the isotropy assumption, the current study is incapable of revealing any orientation dependence of the BDT. Such effects have been observed to play an important role in the BDT [8,15,29,30]. These behaviors can in principal be investigated with the current model, provided that a crystal plasticity theory is used in which only a limited number of slip systems are allowed for dislocation motion. The finite element method for crystal plasticity has been applied by Mohan et al [31,32] to study the crack tip field of FCC single crystals. That approach can readily be adopted in the current model to study the orientation and other structural dependence of the BDT behavior.

Acknowledgments

This work is sponsored by the National Science Foundation through Grant No. MSS 92-09309 RIA. VRN is also supported by a National Science Foundation Graduate Fellowship. The finite element computations using ABAQUS are performed on the Engineering Workstations at the University of Illinois at Urbana-Champaign (UIUC) and on a CRAY Y-MP supercomputer at the National Center for Supercomputing Applications (NCSA), UIUC. The computation on the CRAY Y-MP is partially supported by the NCSA through Grant No. TRA920577N. Helpful discussions with Professors Z. Suo, C.-F. Shih and A. Needleman are gratefully acknowledged.

References

1. J. R. Rice and R. Thomson, *Phil. Mag., 29* (1974) 73.

2. A. S. Argon, *Acta metall., 35* (1987) 185.

3. M. Brede, K. J. Hsia and A. S. Argon, *J. Appl. Phys., 70* (1991) 758.

4. P. B. Hirsch and S. G. Roberts, *Phil. Mag. A, 64* (1991) 55.

5. C. St. John, *Phil. Mag., 32* (1975) 1193.

6. M. Brede and P. Haasen, *Acta metall., 36* (1988) 2003.

7. G. Michot, *Crystal Prop. and Preparation, 17/18* (1988) 55.

8. J. Samuels and S. G. Roberts, *Proc R. Soc. London, A421* (1989) 1.

9. K. J. Hsia and A. S. Argon, "Experimental Study of Micromechanisms of Brittle-to-Ductile Transition in Si Single Crystals", presented at *the 4th International Conference on Fundamentals of Fracture*, Urabandai, Japan, May 31 to June 4, 1993.

10. D. K. Dewald, T. C. Lee, I. M. Robertson, and H. K. Birnbaum, *Scripta Metall., 23* (1989) 1307.

11. J. R. Rice, *J. Mech. Phys. Solids, 40* (1992) 239.

12. J. R. Rice, G. E. Beltz and Y. Sun, in A. S. Argon (ed.), *Topics in Fracture and Fatigue for Materials*, Springer-Verlag, (1992) 1.

13. K. S. Cheung, A. S. Argon, and S. Yip, *J. Appl. Phys., 69* (1991) 2088.

14. M. F. Ashby and J. D. Embury, *Scripta Metall., 19* (1985) 557.

15. P. B. Hirsch, S. G. Roberts, and J. Samuels, *Proc. R. Soc. London, A421* (1989) 25.

16. M. Brede, *Acta Metall. Mater., 41* (1993) 211.

17. D. Hull, *Introduction to Dislocations*, 2nd ed., Pergamon Press, 1975.

18. H. Riedel and J. R. Rice, *Fracture Mechanics: Twelfth Conference, ASTM STP 700*, ASTM,(1980) 112.

19. J. W. Hutchinson, *J. Mech. Phys. Solids, 16* (1968) 13.

20. J. R. Rice and G. F. Rosengran, *J. Mech. Phys. Solids, 16* (1968) 1.

21. J. R. Rice, in H. A. Liebowitz (ed.), *Treatise on Fracture*, Academic Press, 2 (1968) 191.

22. J. D. Landes and J. A. Begley, *Mechanics of Crack Growth, ASTM STP 590*, ASTM (1976) 128.

23. J. L. Bassani and F. A. McClintock, *Solids and Structures, 17* (1981) 479.

24. Z. Suo, C. F. Shih, and A. G. Varias, *Acta Metall. Mater., 41* (1993) 1551.

25. Hibbit, Karlson, and Sorenson, Inc., ABAQUS Version 4.9 (1993).

26. G. Michot and A. George, in S. G. Roberts (ed.), *Proc. 6th Int. Conf. on Dislocations in Semiconductors, IOP Conference Series, 104* (1989) 385.

27. D. Hull, P. Beardmore and A. P. Valintine, *Phil. Mag., 12* (1965) 1021.

28. P. D. Warren, *Scripta Met., 23* (1989) 637.

29. J. S. Wang and P. M. Anderson, *Acta metall., 39* (1991) 779.

30. G. E. Beltz and J. S. Wang, *Acta Metall. Mater., 40* (1992) 1675.

31. R. Mohan, M. Ortiz and C.-F. Shih, *J. Mech Phys. Solids, 40* (1992) 291.

32. R. Mohan, M. Ortiz and C.-F. Shih, *J. Mech. Phys. Solids, 40* (1992) 315.

Table 1: Material constants for *Si* used in calculations

E (GPa)	ν	K_{Ic} $(MPa\sqrt{m})$	Q (eV)	n	σ_0 (MPa)	t_c $(second)$	α
156	0.215	0.9	2.07	1.4	156	50	4.646×10^{-4}

Figure Captions

Figure 1: Typical behavior of the applied stress intensity at temperatures within about 100 degress celsius of the BDT temperature.

Figure 2: Model configuration considered in the current study: (a) circular crack tip region with an elastic zone; (b) the finite element mesh used in the current study.

Figure 3: K_I^{app}/K_{Ic} for different temperatures at a constant normalized loading rate of 1.0. The material parameters used were σ_0/E=0.001, ν= 0.215, Q=1.7 eV, n=1.4, t_c=50 sec., and D/R_0=0.1.

Figure 4: K_I^{tip}/K_{Ic} versus K_I^{app}/K_{Ic} for different loading rates at a constant temperature of T=1000K.

Figure 5: K_I^{app}/K_{Ic} at fracture versus T for different loading rates. the BDT temperature is a function of loading rate.

Figure 6: K_I^{app}/K_{Ic} at fracture versus T for diffferent n at normalized loading rates of 1.0, 5.0 and 10.0.

Figure 7: K_I^{tip}/K_{Ic} versus K_I^{app}/K_{Ic} for different n.

Figure 8: Comparison of our model predicted BDT temperatures with the experimental results of Brede and Haasan [6] for several loading rates. The solid line is the best fit for their experimental data.

Figure 9: Comparison of the applied stress intensity at fracture predicted by our computations with the experimentally measured data of Brede and Haasen [6] for three loading rates.

Figure 10: von Mises stress distribution in the plastic zone at T=T_c for two different loading rates.

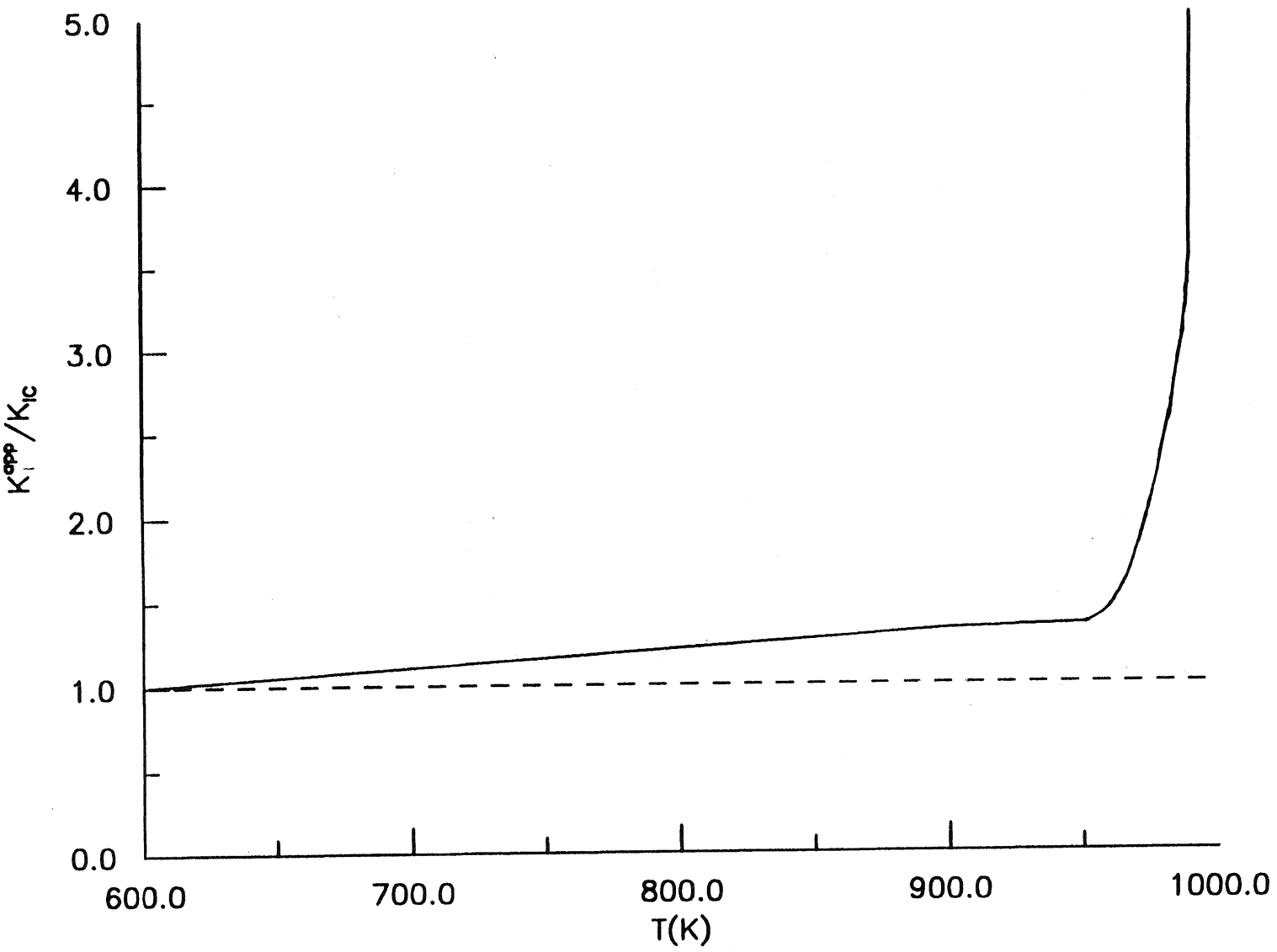

Figure 1

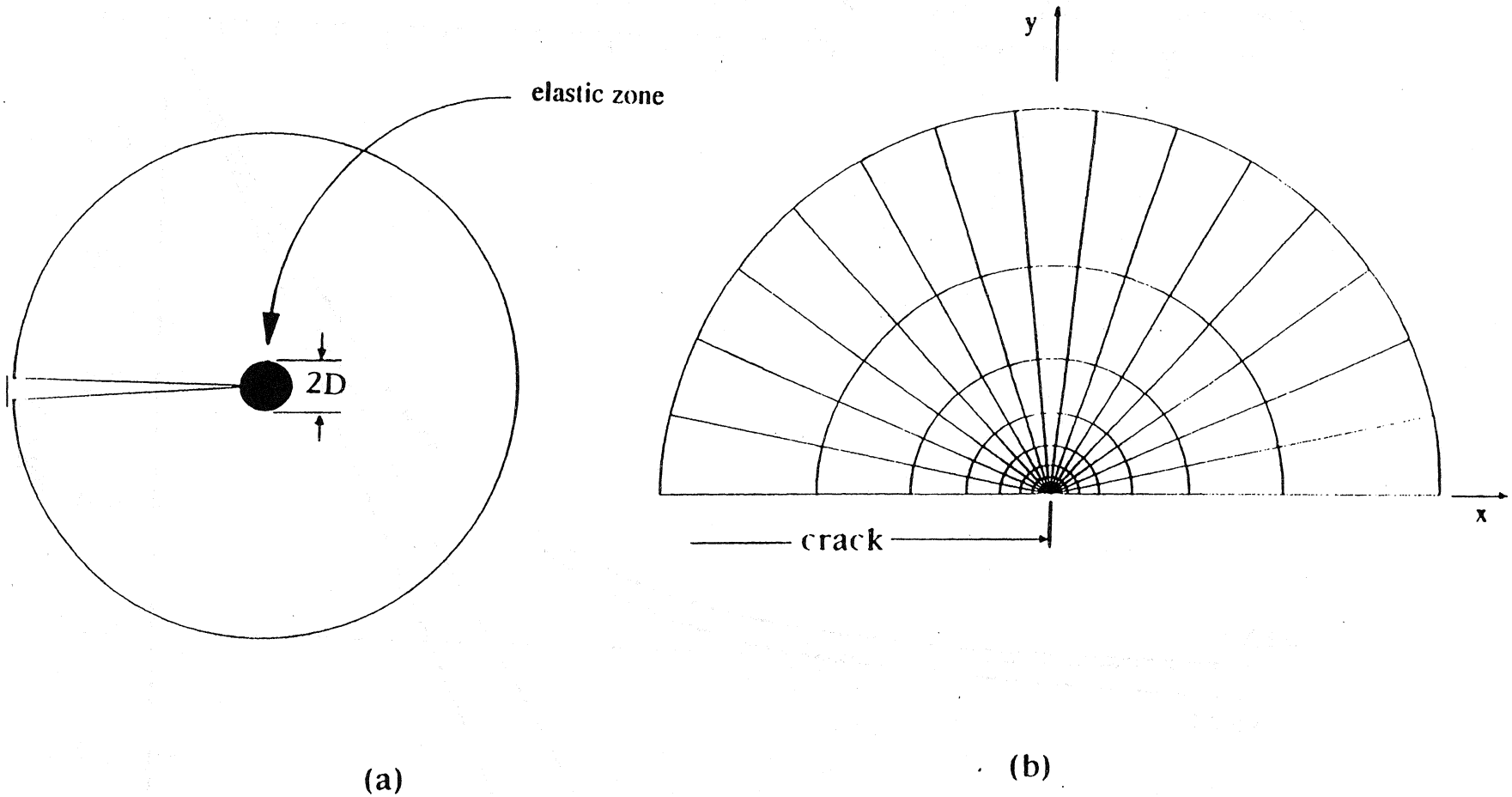

Figure 2

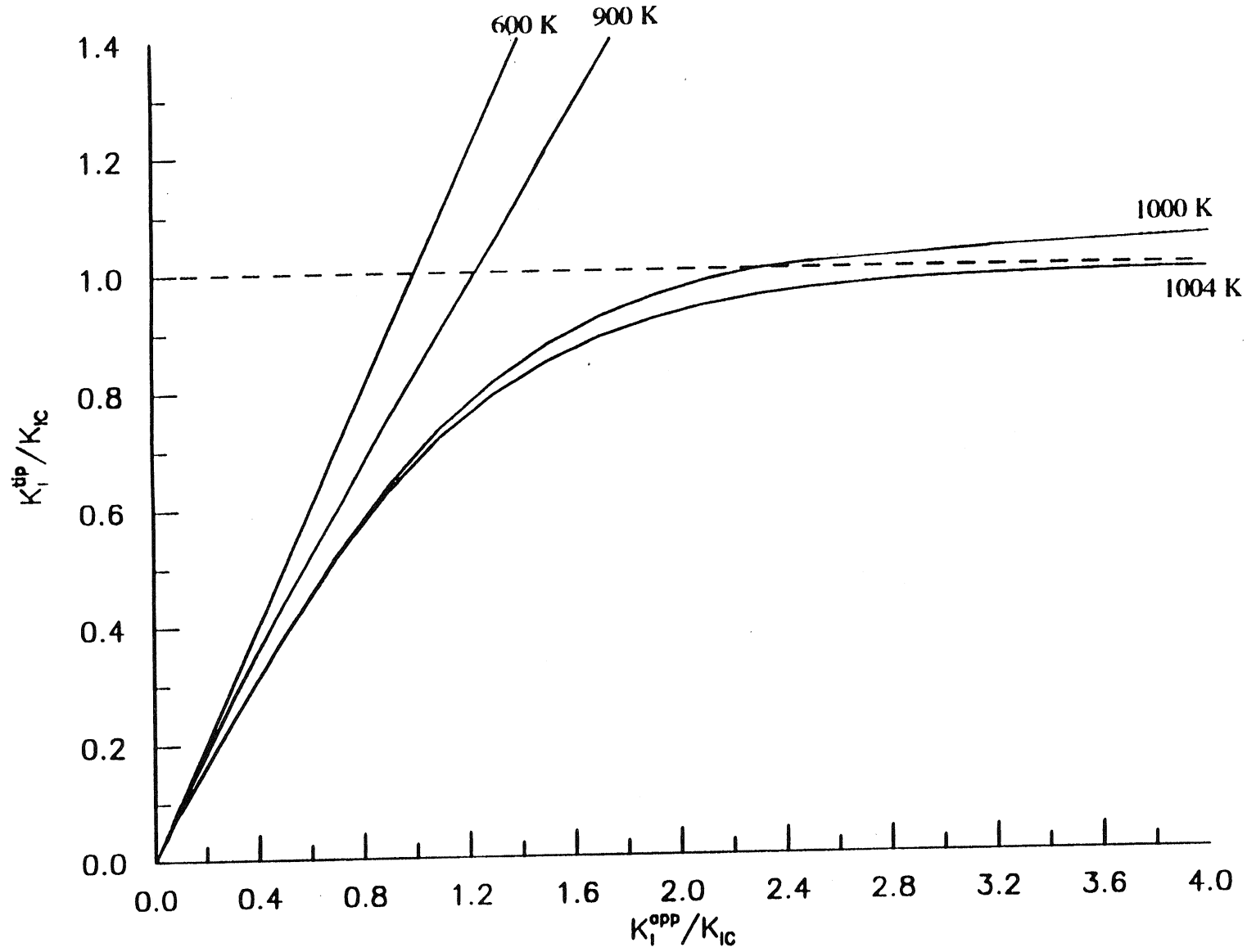
600 K
900 K
1000 K
1004 K
1.4
1.2
1.0
0.8
0.6
0.4
0.2
0.0
K_I^{tip}/K_{IC}
0.0
0.4
0.8
1.2
1.6
2.0
2.4
2.8
3.2
3.6
4.0
K_I^{app}/K_{IC}

Figure 3

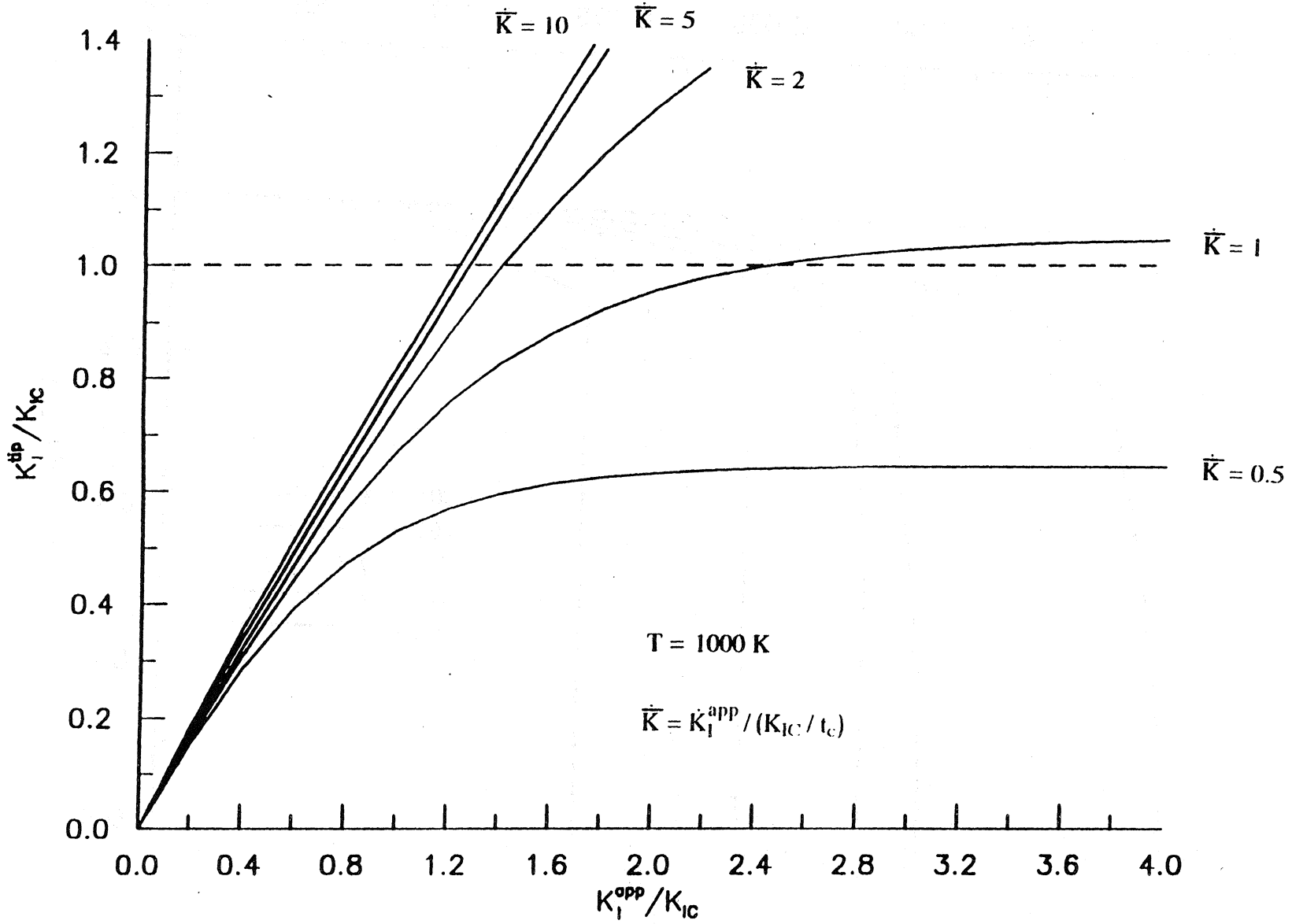
$\dot{K} = 10$
$\dot{K} = 5$
$\dot{K} = 2$
$\dot{K} = 1$
$\dot{K} = 0.5$
T = 1000 K
$\dot{K} = \dot{K}_I^{app} / (K_{IC} / t_c)$
K_I^{dip} / K_{IC}
K_I^{app} / K_{IC}
1.4
1.2
1.0
0.8
0.6
0.4
0.2
0.0
0.0
0.4
0.8
1.2
1.6
2.0
2.4
2.8
3.2
3.6
4.0

Figure 4

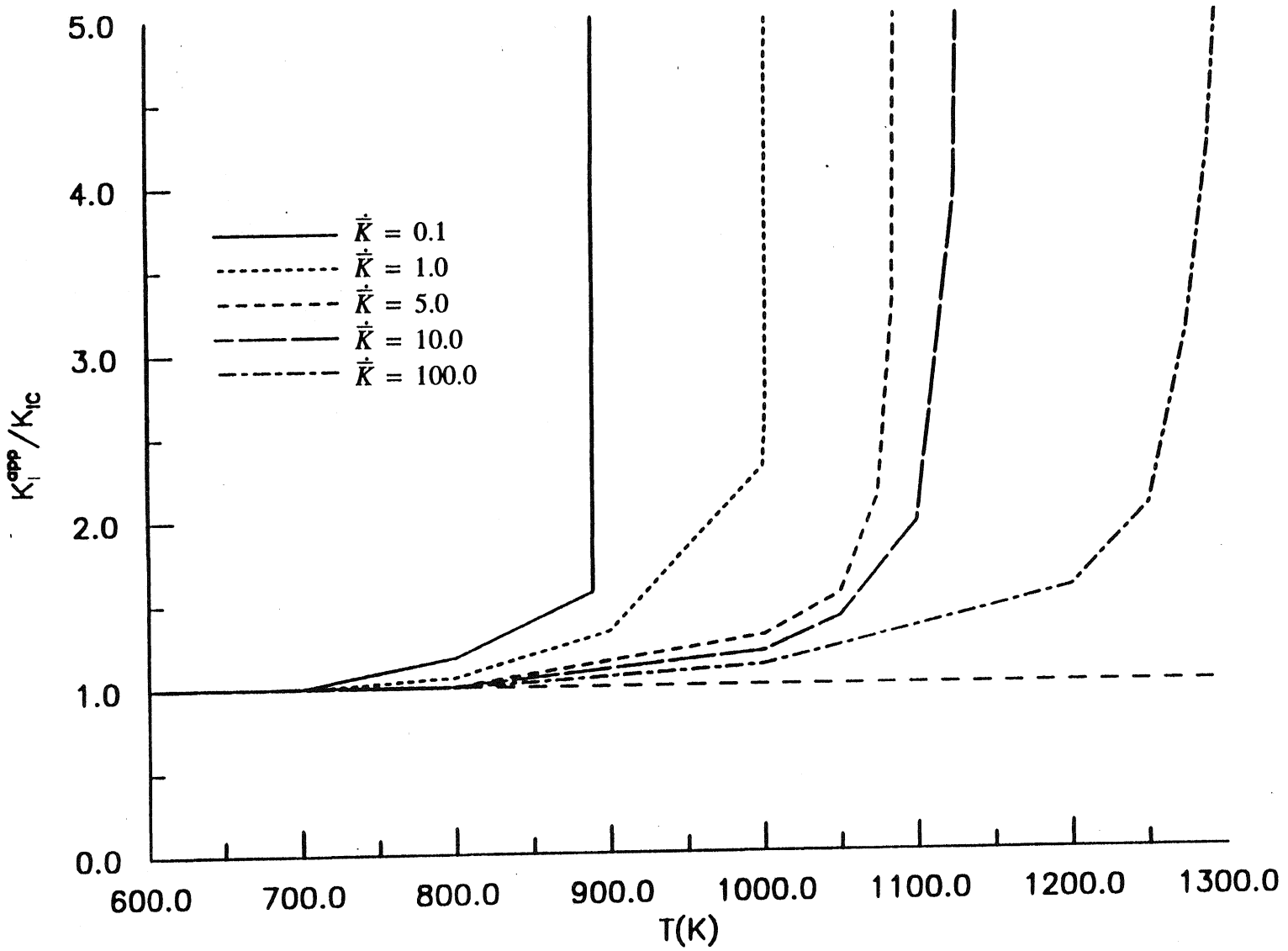
5.0
4.0
3.0
2.0
1.0
0.0
K_I^{app}/K_{Ic}
$\dot{\bar{K}}$ = 0.1
$\dot{\bar{K}}$ = 1.0
$\dot{\bar{K}}$ = 5.0
$\dot{\bar{K}}$ = 10.0
$\dot{\bar{K}}$ = 100.0
600.0
700.0
800.0
900.0
1000.0
1100.0
1200.0
1300.0
T(K)

Figure 5

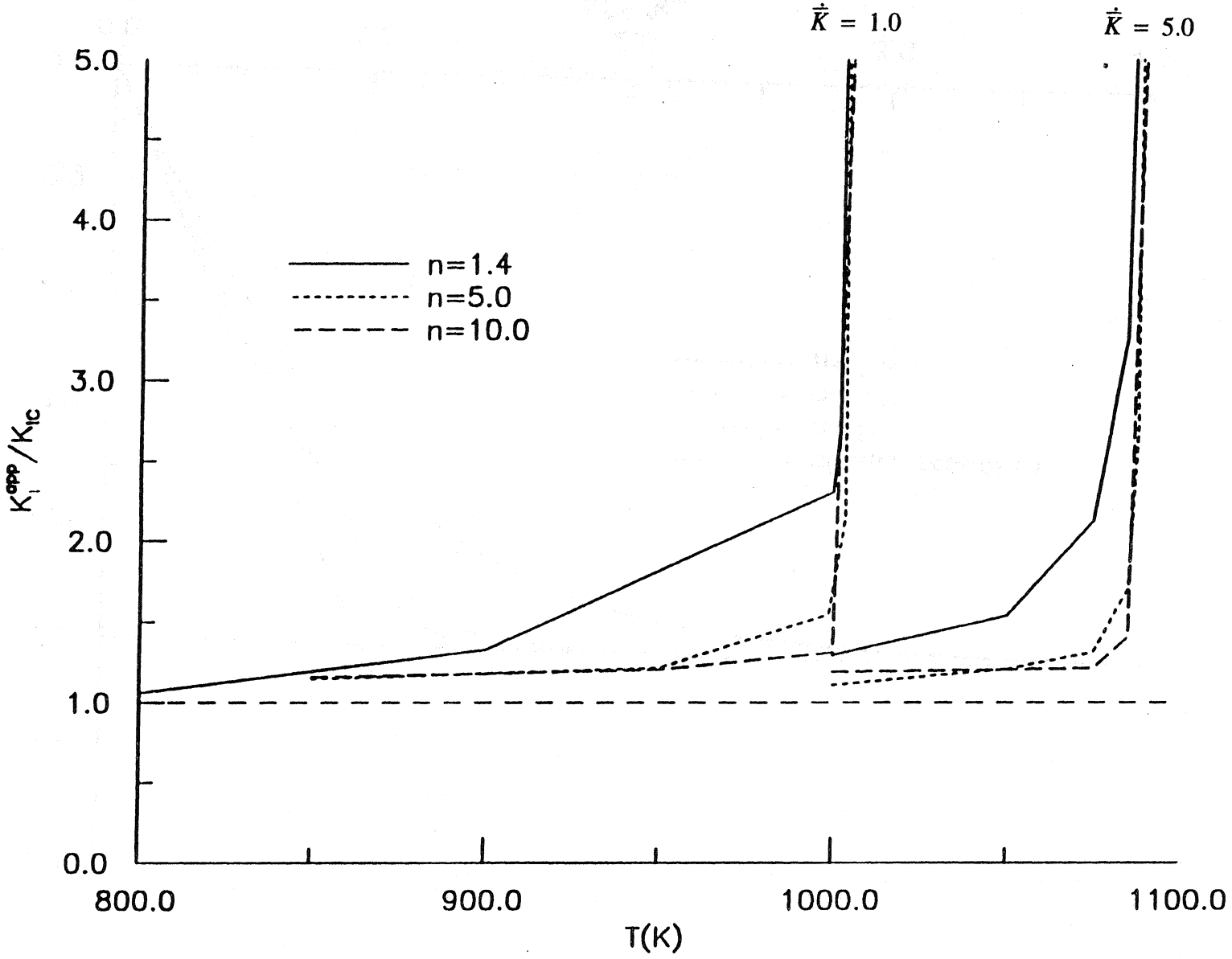
$\dot{\bar{K}}$ = 1.0
$\dot{\bar{K}}$ = 5.0
5.0
4.0
3.0
2.0
1.0
0.0
n=1.4
n=5.0
n=10.0
K_I^{app}/K_{Ic}
800.0
900.0
1000.0
1100.0
T(K)

Figure 6

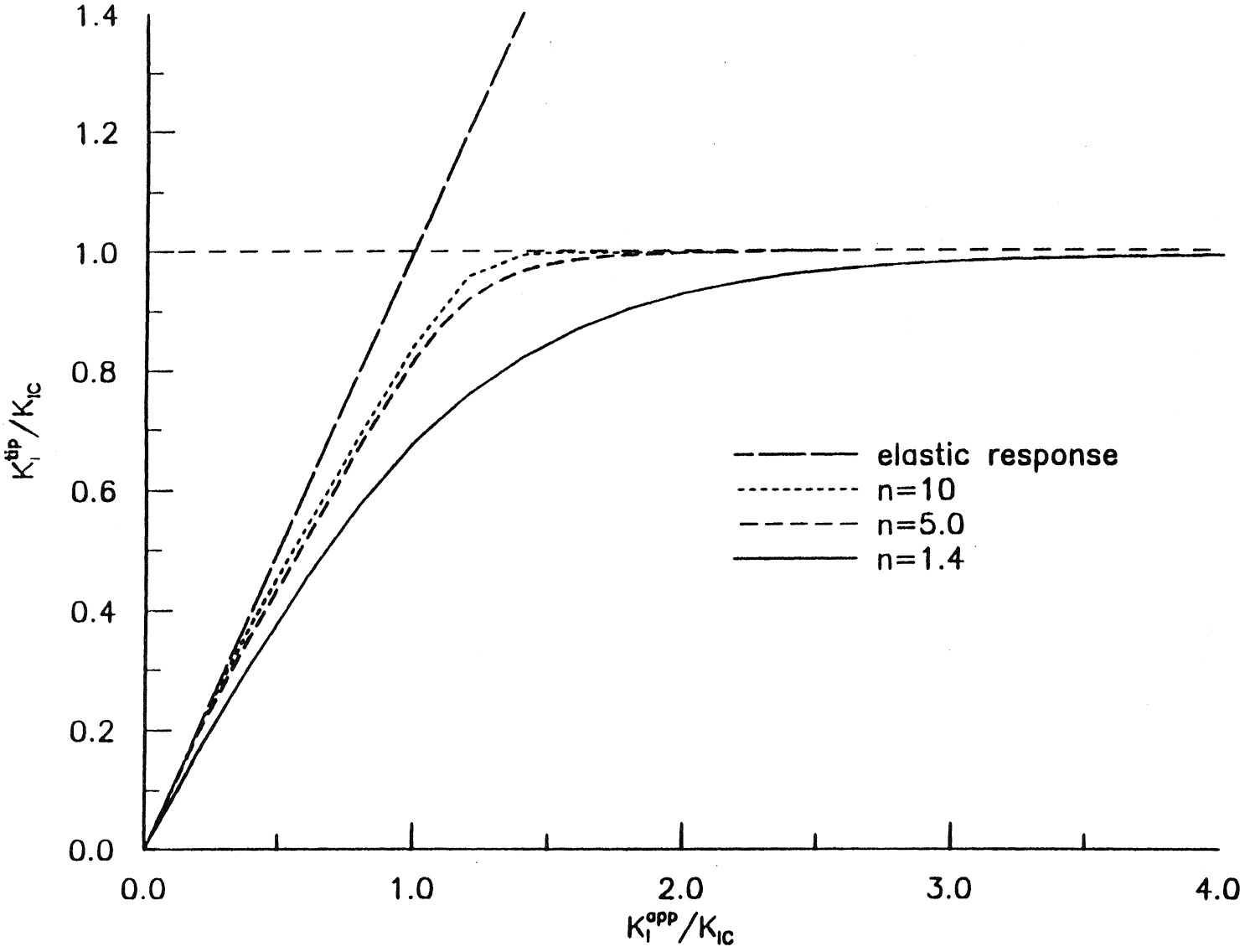
1.4
1.2
1.0
0.8
0.6
0.4
0.2
0.0
K_I^{tip}/K_{IC}
0.0
1.0
2.0
3.0
4.0
K_I^{app}/K_{IC}
elastic response
n=10
n=5.0
n=1.4

Figure 7

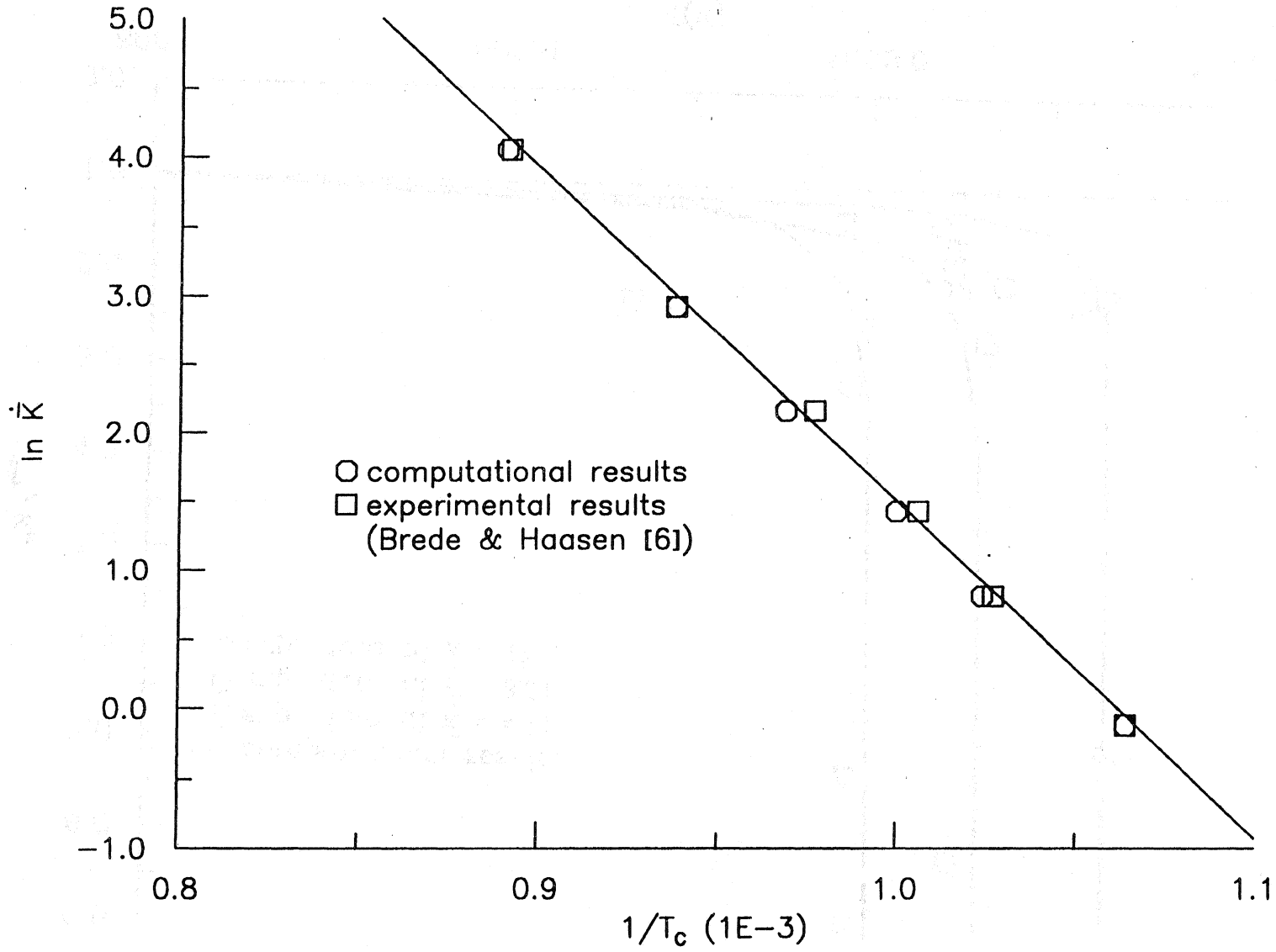
5.0
4.0
3.0
2.0
1.0
0.0
−1.0
ln $\dot{K}$
O computational results
□ experimental results
(Brede & Haasen [6])
0.8
0.9
1.0
1.1
$1/T_c$ (1E−3)

Figure 8

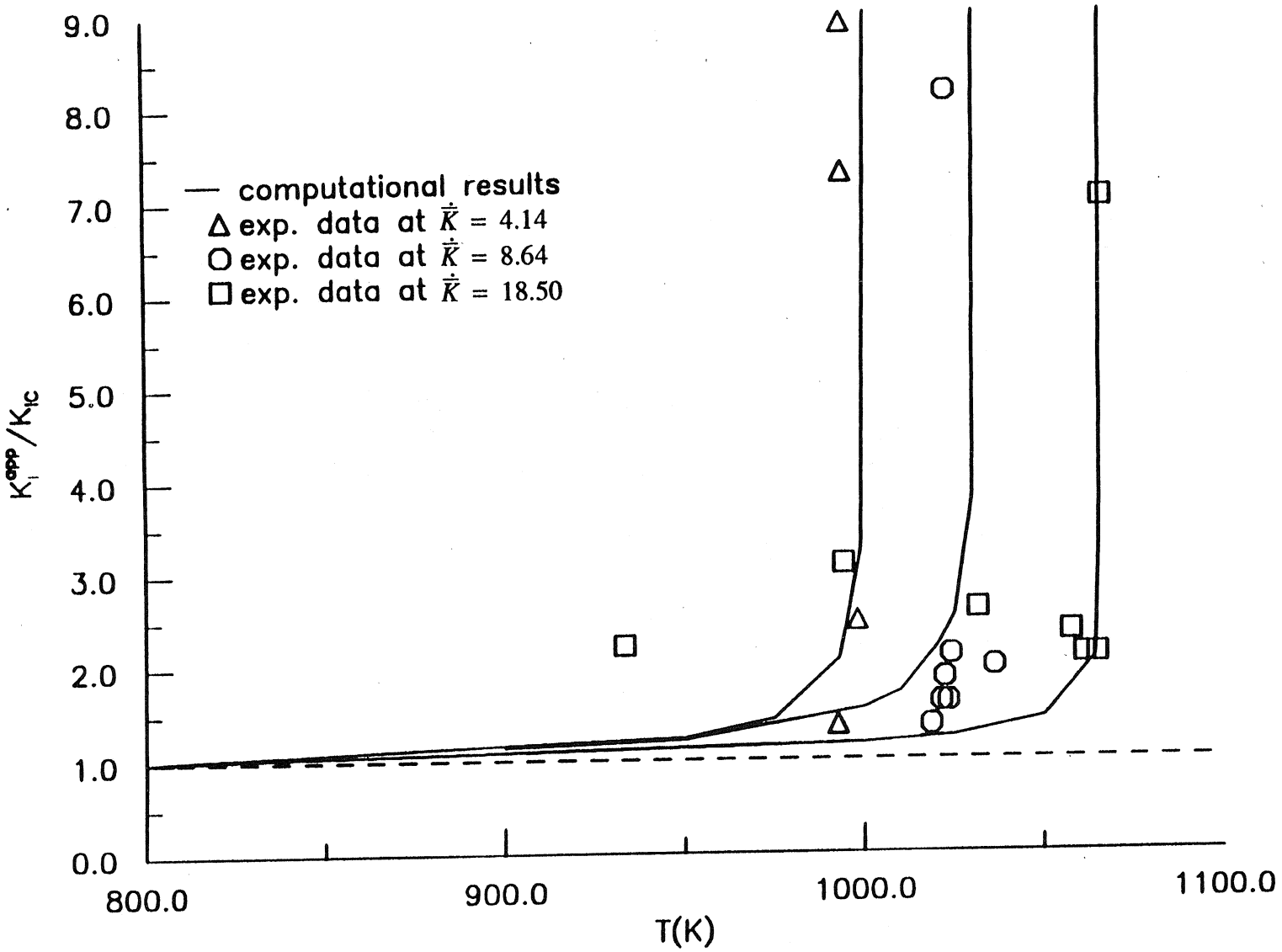
9.0
8.0
7.0
6.0
5.0
4.0
3.0
2.0
1.0
0.0
K_I^{app}/K_{Ic}
— computational results
Δ exp. data at $\dot{\bar{K}}$ = 4.14
O exp. data at $\dot{\bar{K}}$ = 8.64
□ exp. data at $\dot{\bar{K}}$ = 18.50
800.0
900.0
1000.0
1100.0
T(K)

Figure 9

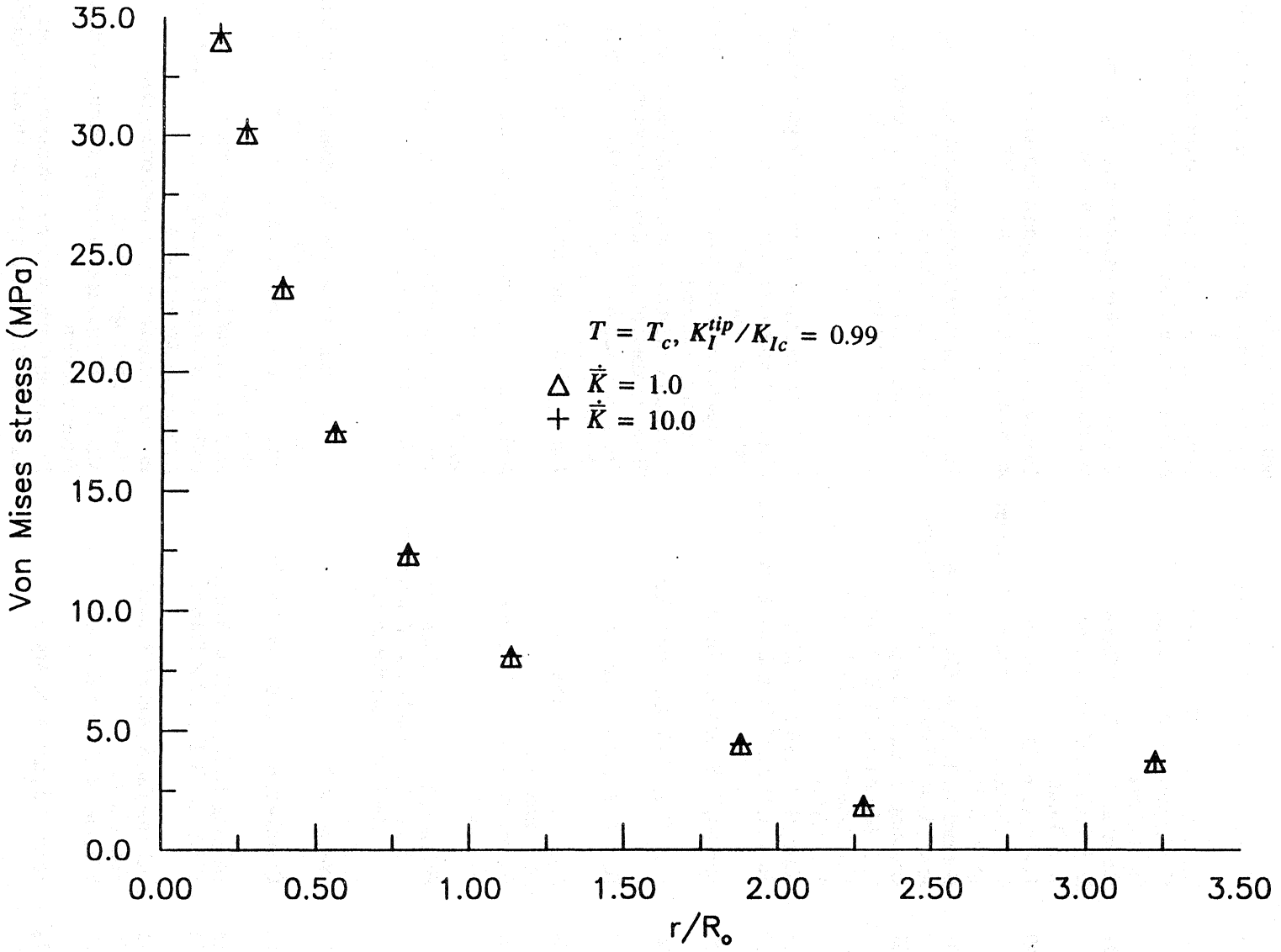
35.0
30.0
25.0
20.0
15.0
10.0
5.0
0.0
Von Mises stress (MPa)
$T = T_c$, $K_I^{tip}/K_{Ic} = 0.99$
$\dot{K} = 1.0$
$\dot{K} = 10.0$
0.00
0.50
1.00
1.50
2.00
2.50
3.00
3.50
r/R$_o$

Figure 10

List of Recent TAM Reports

No.	Authors	Title	Date
494	Toro, J. R.	Existence of weak solutions to the thick plate problem with various boundary conditions	Apr. 1989
495	Stewart, D. S., and B. W. Asay	Discrete modeling of beds of propellant exposed to strong stimulus	Apr. 1991
496	Klein, R., and D. S. Stewart	The relation between curvature, rate state dependence, and detonation velocity	Apr. 1991
497	Powers, J. M., and D. S. Stewart	Approximate solutions for oblique detonations in the hypersonic limit	Apr. 1991
498	Davidson, M. T., K. L. Kuster, K. W. Quinn, N. A. Sluz, and G. Stojkovich	Twenty-fifth student symposium on engineering mechanics, M. E. Clark, coord. (1988)	Feb. 1992
499	Cardenas, H. E., W. C. Crone, D. J. Scott, G. G. Stewart, and B. F. Tatting	Twenty-sixth student symposium on engineering mechanics, M. E. Clark, coord. (1989)	Mar. 1992
700	Juister, C. E., D. W. Newport, C. S. Payne, J. M. Peters, M. P. Thomas, and J. C. Trovillion	Twenty-seventh student symposium on engineering mechanics, M. E. Clark, coord. (1990)	Apr. 1992
701	Bernard, R. T., D. W. Claxon, J. A. Jones, V. R. Nitzsche, and M. T. Stadtherr	Twenty-eighth student symposium on engineering mechanics, M. E. Clark, coord. (1991)	Apr. 1992
702	Greening, L. E., P. J. Joyce, S. G. Martensen, M. D. Morley, J. M. Ockers, M. D. Taylor, and P. J. Walsh	Twenty-ninth student symposium on engineering mechanics, J. W. Phillips, coord. (1992)	May 1992
703	Kuah, H. T., and D. N. Riahi	Instabilities and transition to chaos in plane wakes	Nov. 1992
704	Stewart, D. S., K. Prasad, and B. W. Asay	Simplified modeling of transition to detonation in porous energetic materials	Nov. 1992
705	Stewart, D. S., and J. B. Bdzil	Asymptotics and multi-scale simulation in a numerical combustion laboratory	Jan. 1993
706	Hsia, K. J., Y.-B. Xin, and L. Lin	Numerical simulation of semi-crystalline Nylon 6: Elastic constants of crystalline and amorphous parts	Jan. 1993
707	Hsia, K. J., and J. Q. Huang	Curvature effects on compressive failure strength of long fiber composite laminates	Jan. 1993
708	Jog, C. S., R. B. Haber, and M. P. Bendsoe	Topology design with optimized, self-adaptive materials	Mar. 1993
709	Barkey, M. E., D. F. Socie, and K. J. Hsia	A yield surface approach to the estimation of notch strains for proportional and nonproportional cyclic loading	Apr. 1993
710	Feldsien, T. M., A. D. Friend, G. S. Gehner, T. D. McCoy, K. V. Remmert, D. L. Riedl, P. L. Scheiberle, and J. W. Wu	Thirtieth student symposium on engineering mechanics, J. W. Phillips, coord. (1993)	Apr. 1993
711	Weaver, R. L.	Anderson localization in the time domain: Numerical studies of waves in two-dimensional disordered media	Apr. 1993
712	Cherukuri, H. P., and T. G. Shawki	An energy-based localization theory: Part I—Basic framework	Apr. 1993
713	Manring, N. D., and R. E. Johnson	Modeling a variable-displacement pump	June 1993
714	Birnbaum, H. K., and P. Sofronis	Hydrogen-enhanced localized plasticity—A mechanism for hydrogen-related fracture	July 1993
715	Balachandar, S., and M. R. Malik	Inviscid instability of streamwise corner flow	July 1993
716	Sofronis, P.	Linearized hydrogen elasticity	July 1993
717	Nitzsche, V. R., and K. J. Hsia	Modelling of dislocation mobility controlled brittle-to-ductile transition	July 1993
718	Hsia, K. J., and A. S. Argon	Experimental study of the mechanisms of brittle-to-ductile transition of cleavage fracture in silicon single crystals	July 1993
719	Cherukuri, H. P., and T. G. Shawki	An energy-based localization theory: Part II—Effects of the diffusion, inertia and dissipation numbers	Aug. 1993